Diverging length scale of the inhomogeneous mode-coupling theory: a numerical investigation

Grzegorz Szamel and Elijah Flenner
Department of Chemistry, Colorado State University, Fort Collins, CO 80523
(Dated: December 8, 2009)

Biroli *et al.*'s extension of the standard mode-coupling theory to inhomogeneous equilibrium states [Phys. Rev. Lett. **97**, 195701 (2006)] allowed them to identify a characteristic length scale that diverges upon approaching the mode-coupling transition. We present a numerical investigation of this length scale. To this end we derive and numerically solve equations of motion for coefficients in the small q expansion of the dynamic susceptibility $\chi_{\mathbf{q}}(\mathbf{k};t)$ that describes the change of the system's dynamics due to an external inhomogeneous potential. We study the dependence of the characteristic length scale on time, wave-vector, and on the distance from the mode-coupling transition. We verify scaling predictions of Biroli *et al.* In addition, we find that the numerical value of the diverging length scale qualitatively agrees with lengths obtained from four-point correlation functions. We show that the diverging length scale has very weak k dependence, which contrasts with very strong k dependence of the $q \to 0$ limit of the susceptibility, $\chi_{\mathbf{q}=0}(\mathbf{k};t)$. Finally, we compare the diverging length obtained from the small q expansion to that resulting from an isotropic approximation applied to the equation of motion for the dynamic susceptibility $\chi_{\mathbf{q}}(\mathbf{k};t)$.

PACS numbers:

I. INTRODUCTION

As a liquid is cooled, its dynamics not only gets slower but also becomes increasingly heterogeneous [1, 2, 3]. Moreover, the characteristic size of regions with dynamics both significantly faster and significantly slower than the average dynamics grows upon cooling. This observation has led to the definition of a dynamic correlation length that measures the size of these so-called dynamic heterogeneneities. The dynamic correlation length was defined in terms of a four-point correlation function [4] or a corresponding four-point structure factor [5, 6, 7, 8].

While various four-point functions can readily be obtained from simulations (albeit they typically require more computational effort than the familiar two-point functions), they are difficult to access experimentally. To the best of our knowledge, four-point functions have been obtained directly only from experiments on granular systems [9, 10]. In a remarkable development, Berthier *et al.* [11] showed that derivatives of standard two-point functions with respect to thermodynamic variables like, *e.g.*, density or temperature, could be related to integrals of three-point correlation functions. This opened a door to experimental investigations of the overall degree (the strength) of dynamic heterogeneity upon approaching the glass transition [12]. It should be emphasized, however, that Berthier *et al.* could obtain the dynamic correlation length characterizing the spatial extent of dynamic heterogeneneities only by using additional assumptions that related the integrals of various three-point functions to characteristic length scales exhibited by these functions.

While theoretical understanding of the derivatives of two-point functions with respect to thermodynamic variables is limited, Biroli *et al.* [13] showed that the mode-coupling theory could be used to analyze a closely related quantity, a three-point susceptibility $\chi_{\mathbf{q}}(\mathbf{k};t)$, which describes the change of the intermediate scattering function due to an inhomogeneous external potential. The advantage of this approach is that it allows one to evaluate a characteristic length scale which, up to that time, had remained hidden within the well-known mode-coupling framework. This was possible due to the fact that Biroli *et al.* considered a *non-uniform* external perturbation rather than a uniform change of density or temperature.

To analyze the three-point susceptibility Biroli *et al.* extended the standard mode-coupling theory to describe the time evolution of the intermediate scattering function of a system under the influence of an inhomogeneous external potential. They defined the three-point susceptibility $\chi_{\mathbf{q}}(\mathbf{k};t)$ as a derivative of the intermediate scattering function with respect to a Fourier component of the external potential, $U(\mathbf{q})$. Biroli *et al.* showed that upon approaching the mode-coupling transition both the $q \to 0$ limit of the three-point susceptibility and a characteristic length defined through the small q-dependence of $\chi_{\mathbf{q}}(\mathbf{k};t)$ diverge. Moreover, they derived scaling predictions for the time-dependence of the characteristic length, and they found that this length grows as $t^{a/2}$ in the early β regime (here a is the mode-coupling exponent describing approach of the intermediate scattering function to its plateau value) and then saturates in the late β and α regimes. This was contrasted with the time dependence of the $q \to 0$ limit of the three-point susceptibility which grows as t^a and t^b in the early and late β regimes, respectively (here b is the so-called von Schweidler exponent of the mode-coupling theory describing departure of the intermediate scattering function from its plateau value), peaks around the α relaxation time, and then decays to zero. The strikingly different time-dependence of the characteristic length and the $q \to 0$ limit of the three-point susceptibility was interpreted as an indication of changing fractal dimension of dynamic heterogeneities.

Biroli *et al.* derived only scaling predictions for the three-point susceptibility $\chi_{\mathbf{q}}(\mathbf{k};t)$. They verified some of these predictions through a numerical analysis of a schematic model that completely disregards k dependence. Here we present a numerical investigation of the small q behavior of the three-point susceptibility and the associated characteristic length. We focus on the time and k dependence of the length, and on its dependence on the distance to the mode-coupling transition.

We start with a definition of the three-point susceptibility $\chi_{\mathbf{q}}(\mathbf{k};t)$ in Sec. II. Next, we postulate an expansion of the three-point susceptibility $\chi_{\mathbf{q}}(\mathbf{k};t)$ in powers of $\mathbf{q}$ and derive equations of motion for the first few coefficients in this expansion (see Sec. III). We also present an alternative approach to a numerical evaluation of the characteristic length which is based on an isotropic approximation to the equation of motion (see Sec. IV). Next, in Secs. V and VII we describe the results of the numerical calculations based on the small q expansion and the isotropic approximation, respectively. We finish with a summary and conclusions in Sec. VIII.

II. THREE-POINT SUSCEPTIBILITY $\chi_{\mathbf{q}}(\mathbf{k};t)$

To obtain the equation of motion for the three-point susceptibility Biroli *et al.* [13] considered a Newtonian fluid subject to a periodic in space external potential, derived mode-coupling equation of motion for the intermediate scattering function of this inhomogeneous system, and then differentiated this equation with respect to the external potential. Subsequently, one of us has derived the equation of motion for the same three-point susceptibility for a Brownian system [14]. Not surprisingly, the overdamped limit of the equation of motion derived by Biroli *et al.* coincides with the equation of motion derived starting directly from Brownian dynamics. In this work we will use the latter equation.

For a system subject to a non-uniform external potential the intermediate scattering function is not diagonal in the wave-vector,

$$F(\mathbf{k}_1,\mathbf{k}_2;t) = \frac{1}{N}\left\langle \rho(\mathbf{k}_1;t)\rho(-\mathbf{k}_2)\right\rangle_U . \tag{1}$$

Here $\rho(\mathbf{k}_1;t)$ is the Fourier transform of the microscopic density,

$$\rho(\mathbf{k}_1;t) = \sum_j e^{-i\mathbf{k}_1\cdot\mathbf{r}_j(t)} \tag{2}$$

with $\mathbf{r}_j(t)$ being the position of the jth particle at time t. Furthermore, in Eq. (1) $\rho(\mathbf{k}_1) \equiv \rho(\mathbf{k}_1;t=0)$ and $\langle ...\rangle_U$ denotes the equilibrium average for a system subject to a static non-uniform external potential U.

The three-point susceptibility $\chi_{\mathbf{q}}(\mathbf{k};t)$ is defined through an expansion of the intermediate scattering function in powers of a harmonic external potential $U_{\mathbf{q}} = U_0 e^{-i\mathbf{q}\cdot\mathbf{r}}$,

$$F(\mathbf{k},\mathbf{k}_1;t) = F(k;t)\delta_{\mathbf{k},\mathbf{k}_1} + \chi_{\mathbf{q}}(\mathbf{k};t)\left(-\beta U_0\right)\delta_{\mathbf{k}+\mathbf{q},\mathbf{k}_1} + ... \tag{3}$$

For a system with Brownian dynamics, the equation of motion for the three-point susceptibility $\chi_{\mathbf{q}}(\mathbf{k};t)$ has the following form:

$$\begin{aligned}&\partial_t\chi_{\mathbf{q}}(\mathbf{k};t) + \frac{D_0k^2}{S(k)}\chi_{\mathbf{q}}(\mathbf{k};t)\\ &+\int_0^t dt' M^{\rm irr}(k;t-t')\partial_{t'}\chi_{\mathbf{q}}(\mathbf{k};t')\\ &+\int_0^t dt' M^{\chi}_{\mathbf{q}}(\mathbf{k};t-t')\partial_{t'}F(|\mathbf{k}+\mathbf{q}|;t')\\ &= \mathcal{S}_{\mathbf{q}}(\mathbf{k};t)\end{aligned} \tag{4}$$

In Eq. (4) D_0 is the diffusion coefficient of an isolated particle, $S(k)$ denotes the static structure factor, $M^{\rm irr}(k;t)$ is the irreducible memory function of mode-coupling theory,

$$\begin{aligned}&M^{\rm irr}(k;t) =\\ &\frac{nD_0}{2}\int\frac{d\mathbf{k}_1}{(2\pi)^2}[v_{\mathbf{k}}(\mathbf{k}_1,\mathbf{k}-\mathbf{k}_1)]^2F(k_1;t)F(|\mathbf{k}-\mathbf{k}_1|;t),\end{aligned} \tag{5}$$

and $M^{\chi}(\mathbf{q},k;t)$ is defined as follows,

$$\begin{aligned}&M^{\chi}_{\mathbf{q}}(\mathbf{k};t) = \frac{nD_0k}{|\mathbf{k}+\mathbf{q}|}\int\frac{d\mathbf{k}_1}{(2\pi)^3}v_{\mathbf{k}}(\mathbf{k}_1,\mathbf{k}-\mathbf{k}_1)\\ &\times\chi_{\mathbf{q}}(\mathbf{k}_1;t)F(|\mathbf{k}-\mathbf{k}_1|;t)v_{\mathbf{k}+\mathbf{q}}(\mathbf{k}_1+\mathbf{q},\mathbf{k}-\mathbf{k}_1).\end{aligned} \tag{6}$$

In Eqs. (5-6) $v_{\mathbf{k}}(\mathbf{k}_1,\mathbf{k}_2) = \hat{\mathbf{k}}\cdot(\mathbf{k}_1c(k_1) + \mathbf{k}_2c(k_2))$ with $\hat{\mathbf{k}} = \mathbf{k}/k$, and n is the density. The source term in Eq. (4), $\mathcal{S}_{\mathbf{q}}(\mathbf{k};t)$, is given by

$$\begin{aligned}&\mathcal{S}_{\mathbf{q}}(\mathbf{k};t) =\\ &D_0k^2S(q)\left(1-\frac{\mathbf{k}\cdot(\mathbf{k}+\mathbf{q})}{k^2S(|\mathbf{k}+\mathbf{q}|)}\right)F(|\mathbf{k}+\mathbf{q}|;t)\\ &+S(q)\int_0^t dt' M^{\rm irr}(k;t-t')\frac{\mathbf{k}\cdot(\mathbf{k}+\mathbf{q})}{|\mathbf{k}+\mathbf{q}|^2}\partial_{t'}F(|\mathbf{k}+\mathbf{q}|;t').\end{aligned} \tag{7}$$

Finally, the initial condition for the three-point susceptibility is $\chi_{\mathbf{q}}(\mathbf{k};t=0) = S(k)S(q)S(|\mathbf{k}+\mathbf{q}|)$. This form of the initial condition is obtained by applying a convolution approximation to the exact expression for the initial condition, which involves a three-particle correlation function. One should note that the same convolution approximation is used in the derivation of the mode-coupling equation of motion (both in a uniform and a non-uniform equilibrium state).

It should be emphasized at this point that solving Eq. (4) numerically is considerably more involved than solving the uniform equilibrium mode-coupling equations [15, 16, 17], and, to the best of our knowledge, has never been attempted. The reason is that while $\mathbf{q}$ is a parameter in Eq. (4), non-zero value of $\mathbf{q}$ breaks rotational symmetry. Thus, $\chi_{\mathbf{q}}(\mathbf{k};t)$ depends not only on $k = |\mathbf{k}|$ and $q = |\mathbf{q}|$, but also on the angle between $\mathbf{k}$ and $\mathbf{q}$. Most importantly, the latter angle is an independent variable, rather than a parameter in Eq. (4).

III. EXPANSION OF $\chi_{\mathbf{q}}(\mathbf{k};t)$

A. Preliminaries

In this work we focus on the characteristic length defined through the small q-dependence of the three-point susceptibility $\chi_{\mathbf{q}}(\mathbf{k};t)$. Thus, to calculate this length we only need to obtain the small q behavior of the susceptibility. We postulate the following expansion of $\chi_{\mathbf{q}}(\mathbf{k};t)$ in powers of $\mathbf{q}$,

$$\begin{aligned}\chi_{\mathbf{q}}(\mathbf{k};t) &= \chi^{(0)}(k;t)+\sum_{\alpha} q_\alpha \left[\frac{\partial \chi_{\mathbf{q}}(\mathbf{k};t)}{\partial q_\alpha}\right]_{\mathbf{q}=0} \\ &\quad +\sum_{\alpha\beta}\frac{q_\alpha q_\beta}{2}\left[\frac{\partial^2\chi_{\mathbf{q}}(\mathbf{k};t)}{\partial q_\alpha \partial q_\beta}\right]_{\mathbf{q}=0}+\dots \\ &= \chi^{(0)}(k;t)+\hat{\mathbf{k}}\cdot\mathbf{q}\chi^{(1)}(k;t) \\ &\quad +\mathbf{q}^2\chi^{(2)}(k;t) \\ &\quad +\left(3\left(\hat{\mathbf{k}}\cdot\mathbf{q}\right)^2-\mathbf{q}^2\right)\chi^{(2)}_{\rm tl}(k;t)+\dots \quad (8)\end{aligned}$$

where the second equality follows from symmetry considerations and quantities $\chi^{(1)}$, $\chi^{(2)}$, and $\chi^{(2)}_{\rm tl}$ are defined as follows:

$$\chi^{(1)}(k;t) = \sum_\alpha \hat{k}_\alpha \left.\frac{\partial\chi_{\mathbf{q}}(\mathbf{k};t)}{\partial q_\alpha}\right|_{\mathbf{q}=0} \quad (9)$$

$$\chi^{(2)}(k;t) = \frac{1}{6}\sum_\alpha \left.\frac{\partial^2\chi_{\mathbf{q}}(\mathbf{k};t)}{\partial q_\alpha\partial q_\alpha}\right|_{\mathbf{q}=0} \quad (10)$$

$$\chi^{(2)}_{\rm tl}(k;t) = \frac{1}{4}\sum_{\alpha\beta}\left(\hat{k}_\alpha\hat{k}_\beta-\frac{1}{3}\delta_{\alpha\beta}\right)\left.\frac{\partial^2\chi_{\mathbf{q}}(\mathbf{k};t)}{\partial q_\alpha q_\beta}\right|_{\mathbf{q}=0} \quad (11)$$

We show in Sec. V that the first order term, $\chi^{(1)}(k;t)$, does not lead to a diverging characteristic length scale. Furthermore, we show that the second order term originating from the trace of the second derivative of $\chi_{\mathbf{q}}(\mathbf{k};t)$, $\chi^{(2)}(k;t)$, leads to a diverging characteristic length scale. Finally, it can be shown that the second order term originating from the symmetric traceless part of the second derivative of $\chi_{\mathbf{q}}(\mathbf{k};t)$, $\chi^{(2)}_{\rm tl}(k;t)$, does not lead to a diverging characteristic length scale thus we omit the equation of motion for $\chi^{(2)}_{\rm tl}(k;t)$ for sake of space a clarity.

B. Zeroth order coefficient $\chi^{(0)}(k;t)$

To get the equation of motion for $\chi^{(0)}(k;t)$ we need to take $\mathbf{q}\to 0$ limit in all terms in Eq. (4). In this way we obtain the following equation,

$$\begin{aligned}&\partial_t\chi^{(0)}(k;t)+D_0\frac{k^2}{S(k)}\chi^{(0)}(k;t) \\ &\quad +\int_0^t dt' M^{\rm irr}(k;t-t')\partial_{t'}\chi^{(0)}(k;t') \\ &\quad +\int_0^t dt' M_0^{\chi}(k;t-t')\partial_{t'}F(k;t') \\ &= nD_0k^2S(0)c(k)F(k;t) \\ &\quad +S(0)\int_0^t dt' M^{\rm irr}(k;t-t')\partial_{t'}F(k;t') \quad (12)\end{aligned}$$

where

$$\begin{aligned}M_0^{\chi}(k;t) &= nD_0\int\frac{d\mathbf{k}_1}{(2\pi)^3}[v_{\mathbf{k}}(\mathbf{k}_1,\mathbf{k}-\mathbf{k}_1)]^2 \\ &\quad \times\chi^{(0)}(k_1;t)F(|\mathbf{k}-\mathbf{k}_1|;t). \quad (13)\end{aligned}$$

Furthermore, taking $\mathbf{q}\to 0$ limit of the initial condition $\chi_{\mathbf{q}}(\mathbf{k};t=0)=S(k)S(q)S(|\mathbf{k}+\mathbf{q}|)$ we obtain the initial condition for $\chi^{(0)}(k;t)$, $\chi^{(0)}(k;t=0)=S(0)S(k)^2$.

The zeroth order coefficient, $\chi^{(0)}(k;t)$, satisfies essentially the same equation of motion as three point susceptibility $\chi_n(k;t)$, which is defined as the density derivative of the intermediate scattering function [18]. This was expected: in the long wavelength, $\mathbf{q}\to 0$, limit the derivative with respect to the external potential differs from the derivative with respect to the density by a thermodynamic factor proportional to $(\partial n/\partial\beta\mu)_T$.

The equation of motion (12) can be solved using the static structure factor $S(k)$ and the dynamic scattering function $F(k;t)$ as input. We calculate $F(k;t)$ using the mode-coupling theory; the equation of motion for $F(k;t)$ reads,

$$\begin{aligned}\partial_t F(k;t) &+ \frac{D_0k^2}{S(k)}F(k;t) \\ &+ \int_0^t dt' M^{\rm irr}(k;t-t')\partial_{t'}F(k;t')=0, \quad (14)\end{aligned}$$

where $M^{\rm irr}$ is the irreducible memory function given by Eq. (5).

C. First order coefficient $\chi^{(1)}(k;t)$

To get the equation of motion for $\chi^{(1)}(k;t)$ we need to expand all the terms in Eq. (4) in powers of $\mathbf{q}$ and then to collect terms linear in $\mathbf{q}$. After exploiting rotational

symmetry we get the following equation of motion

$$\begin{aligned}
&\partial_t\chi^{(1)}(k;t)+\frac{D_0k^2}{S(k)}\chi^{(1)}(k;t) \qquad (15)\\
&+\int_0^t dt' M^{\rm irr}(k;t-t')\partial_{t'}\chi^{(1)}(k;t')\\
&+\int_0^t dt' M_1^{\chi}(k;t-t')\partial_{t'}F(k;t')\\
&+\int_0^t dt' M_0^{\chi}(k;t-t')\partial_{t'}\partial_k F(k;t')\\
=\;&\frac{D_0S(0)F(k;t)k^2}{S(k)}\left[\frac{1}{S(k)}\frac{dS(k)}{dk}-\frac{1}{k}\right]\\
&+nD_0k^2S(0)c(k)\partial_kF(k;t)\\
&+S(0)\int_0^t dt' M^{\rm irr}(k;t-t')\partial_{t'}\partial_kF(k;t')\\
&-\frac{S(0)}{k}\int_0^t dt' M^{\rm irr}(k;t-t')\partial_{t'}F(k;t'),
\end{aligned}$$

where

$$\begin{aligned}
&M_1^{\chi}(k;t)=\\
&nD_0\int\frac{d\mathbf{k}_1}{(2\pi)^3}[v_{\mathbf{k}}(\mathbf{k}_1,\mathbf{k}-\mathbf{k}_1)]^2\frac{\mathbf{k}\cdot\mathbf{k}_1}{kk_1}\\
&\times F(|\mathbf{k}-\mathbf{k}_1|;t)\chi^{(1)}(k_1;t)\\
&+nD_0\int\frac{d\mathbf{k}_1}{(2\pi)^3}v_{\mathbf{k}}(\mathbf{k}_1,\mathbf{k}-\mathbf{k}_1)F(|\mathbf{k}-\mathbf{k}_1|;t)\chi^{(0)}(k_1;t)\\
&\times\left\{c(k_1)+\frac{[\mathbf{k}\cdot\mathbf{k}_1]^2}{k^2k_1}\frac{dc(k_1)}{dk_1}-\frac{v_{\mathbf{k}}(\mathbf{k}_1,\mathbf{k}-\mathbf{k}_1)}{k}\right\}. \qquad (16)
\end{aligned}$$

Furthermore, we obtain the following expression for the initial condition for $\chi^{(1)}(k;t)$, $\chi^{(1)}(k;t=0)=S(k)S(0)dS(k)/dk$.

To solve Eq. (15) we need the equation of motion for the partial derivative of the intermediate scattering function with respect to the wave-vector, $\partial_kF(k;t)$. This equation can be derived from the mode-coupling equation (14):

$$\begin{aligned}
&\partial_t\partial_kF(k;t)+\frac{D_0k^2}{S(k)}\partial_kF(k;t)\\
&+\frac{D_0k}{S(k)}\left[2-\frac{k}{S(k)}\partial_kS(k)\right]F(k;t)\\
&+\int_0^t dt' M^{\rm irr}(k;t-t')\partial_{t'}\partial_kF(k;t')\\
&+\int_0^t M_1^{k1}(k;t-t')\partial_{t'}F(k;t')\\
&+\int_0^t dt' M_2^{k1}(k;t-t')\partial_{t'}F(k;t')=0 \qquad (17)
\end{aligned}$$

where

$$\begin{aligned}
&M_1^{k1}= \qquad (18)\\
&nD_0\int\frac{d\mathbf{k}_1}{(2\pi)^3}\left[v_{\mathbf{k}}(\mathbf{k}_1,\mathbf{p})\right]\left\{c(p)+\frac{[\mathbf{k}\cdot\mathbf{p}]^2}{k^2p}\frac{dc(p)}{dp}\right\}\\
&\times F(k_1;t)F(p;t),
\end{aligned}$$

and

$$\begin{aligned}
&M_2^{k1}(k;t)= \qquad (19)\\
&\frac{nD_0}{2}\int\frac{d\mathbf{k}_1}{(2\pi)^3}[v_{\mathbf{k}}(\mathbf{k}_1,\mathbf{p})]^2F(k_1;t)\frac{\mathbf{k}\cdot\mathbf{p}}{kp}\partial_pF(p;t).
\end{aligned}$$

In Eqs. (18-19) $\mathbf{p}=\mathbf{k}-\mathbf{k}_1$ and $p=|\mathbf{k}-\mathbf{k}_1|$.

D. Second order coefficient $\chi^{(2)}(k;t)$

For symmetry reasons, there are two linearly independent second order coefficients, the coefficient proportional to the trace of the matrix of second derivatives of $\chi_{\mathbf{q}}(\mathbf{k};t)$, $\chi^{(2)}(k;t)$, and the coefficient proportional to the symmetric traceless part of the matrix of second derivatives of $\chi_{\mathbf{q}}(\mathbf{k};t)$, $\chi^{(2)}_{tl}(k;t)$. It can be shown that only the former coefficient leads to a characteristic length that diverges upon approaching the mode-coupling transition. Therefore, since the focus of this work is the diverging characteristic length, we will only give the equation of motion for $\chi^{(2)}(k;t)$. By expanding equation of motion (4) in powers of $\mathbf{q}$, collecting the second order terms and taking a trace of the corresponding tensorial equation of motion we can derive the following equation of motion for $\chi^{(2)}(k;t)$:

$$\begin{aligned}
&\partial_t\chi^{(2)}(k;t)+D_0\frac{k^2}{S(k)}\chi^{(2)}(k;t)\\
&+\int_0^t dt' M^{\rm irr}(k;t-t')\partial_{t'}\chi^{(2)}(k;t')\\
&+\int_0^t dt' M_2^{\chi}(k;t-t')\partial_{t'}F(k;t')\\
=\;&-\frac{1}{6}\int_0^t dt' M_0^{\chi}(k;t-t')\partial_{t'}\partial_k^2F(k;t')\\
&-\frac{1}{3k}\int_0^t dt' M_0^{\chi}(k;t-t')\partial_{t'}\partial_kF(k;t')\\
&-\frac{2}{3}\int_0^t dt' M_1^{\chi}(k;t-t')\partial_{t'}\partial_kF(k;t')\\
&-\frac{2}{3}\int_0^t dt' M_3^{\chi}(k;t-t')\partial_{t'}F(k;t')\\
&+\mathcal{S}^{(2)}(k;t), \qquad (20)
\end{aligned}$$

where

$$\mathcal{S}^{(2)}(k;t) = \left[\frac{d^2S(q)}{dq^2}\Big|_{q=0}\right]\frac{nD_0k^2c(k)F(k;t)}{2} + \frac{D_0k^2S(0)}{3S(k)^2}\partial_kF(k;t)\left[\frac{dS(k)}{dk}-\frac{S(k)}{k}\right] + \frac{D_0k^2S(0)}{6S(k)^2}F(k;t)\left[\frac{5}{k}\frac{dS(k)}{dk}-\frac{2}{S(k)}\left[\frac{dS(k)}{dk}\right]^2 + \frac{d^2S(k)}{dk^2}\right] + \frac{D_0k^2S(0)nc(k)}{6}\partial_k^2F(k;t) + \frac{1}{3}\left[\frac{d^2S(q)}{dq^2}\Big|_{q=0}-\frac{S(0)}{k^2}\right]\int_0^t dt'M^{\rm irr}(k;t-t')\partial_{t'}F(k;t') + \frac{1}{6}\frac{S(0)}{k}\int_0^t dt'M^{\rm irr}(k;t-t')\partial_{t'}\partial_kF(k;t') + \frac{S(0)}{6}\int_0^t dt'M^{\rm irr}(k;t-t')\partial_{t'}\partial_k^2F(k;t'), \quad (21)$$

and

$$M_2^{\chi}(k;t) = nD_0\int\frac{d\mathbf{k}_1}{(2\pi)^3}[v_{\mathbf{k}}(\mathbf{k}_1,\mathbf{k}-\mathbf{k}_1)]^2 \times F(|\mathbf{k}-\mathbf{k}_1|;t)\chi^{(2)}(k_1;t), \quad (22)$$

and

$$M_3^{\chi}(k;t) = nD_0\int\frac{d\mathbf{k}_1}{(2\pi)^3}v_{\mathbf{k}}(\mathbf{k}_1,\mathbf{p})F(p;t)\chi^{(1)}(k_1;t) \times\left[\frac{v_{\mathbf{k}_1}(\mathbf{k}_1,\mathbf{p})}{k}-\frac{2(\mathbf{k}\cdot\mathbf{k}_1)}{k^2k_1}v_{\mathbf{k}}(\mathbf{k}_1,\mathbf{p})+\frac{\mathbf{k}\cdot\mathbf{k}_1}{k}\frac{dc(k_1)}{dk_1}\right] + \frac{nD_0}{2}\int\frac{d\mathbf{k}_1}{(2\pi)^3}v_{\mathbf{k}}(\mathbf{k}_1,\mathbf{p})F(p;t)\chi^{(0)}(k_1;t) \times\left[\frac{c(k_1)}{k}-\frac{v_{\mathbf{k}}(\mathbf{k}_1,\mathbf{p})}{k^2}+\frac{\mathbf{k}\cdot\mathbf{k}_1}{2k}\frac{d^2c(k_1)}{dk_1^2} -\frac{2(\mathbf{k}\cdot\mathbf{k}_1)^2-2k^2\mathbf{k}\cdot\mathbf{k}_1-k^2k_1^2}{k^3k_1}\frac{dc(k_1)}{dk_1}\right]. \quad (23)$$

In Eq. (23) $\mathbf{p}=\mathbf{k}-\mathbf{k}_1$ and $p=|\mathbf{k}-\mathbf{k}_1|$. The initial condition is given by

$$\chi^{(2)}(k;0) = \frac{S^2(k)}{2}\left[\frac{d^2S(q)}{dq^2}\Big|_{q=0}\right] + \frac{1}{3}\frac{S(k)S(0)}{k}\frac{dS(k)}{dk}+\frac{1}{6}S(k)S(0)\frac{d^2S(k)}{dk^2} \quad (24)$$

To solve Eq. 20 we also need the equation of motion (17) for $\partial_kF(k;t)$ and the equation of motion for the second partial derivative of the intermediate scattering function with respect to the wave-vector, $\partial_k^2F(k;t)$. The latter equation can be obtained from the mode-coupling theory equation of motion, Eq. (14):

$$\partial_t\partial_k^2F(k;t)+\left[\frac{2D_0}{S(k)}-\frac{4D_0k}{S(k)^2}\frac{dS(k)}{dk}\right]F(k;t) -\left[\frac{2}{S(k)}\left(\frac{dS(k)}{dk}\right)^2+\frac{d^2S(k)}{dk^2}\right]\frac{D_0k^2}{S(k)^2}F(k;t) +\left[\frac{4D_0k}{S(k)}-\frac{2D_0k^2}{S(k)^2}\frac{dS(k)}{dk}\right]\partial_kF(k;t) +\frac{D_0k^2}{S(k)}\partial_k^2F(k;t) +\int_0^t dt'M^{\rm irr}(k;t-t')\partial_{t'}\partial_k^2F(k;t') +\int_0^t dt'M_1^{k2}(k;t-t')\partial_{t'}\partial_kF(k;t') +\int_0^t dt'M_2^{k2}(k;t-t')\partial_{t'}F(k;t') = 0, \quad (25)$$

where

$$M_1^{k2}(k;t) = 2nD_0\int\frac{d\mathbf{k}_1}{(2\pi)^3}v_{\mathbf{k}}(\mathbf{k}_1,\mathbf{p})\left\{c(p)+\frac{[\mathbf{k}\cdot\mathbf{p}]^2}{k^2p}\frac{dc(p)}{dp}\right\} \times F(k_1;t)F(p;t), +nD_0\int\frac{d\mathbf{k}_1}{(2\pi)^3}[v_{\mathbf{k}}(\mathbf{k}_1,\mathbf{p})]^2\frac{\mathbf{k}\cdot\mathbf{p}}{kp}\partial_pF(p;t-t')F(k_1;t) \quad (26)$$

and

$$M_2^{k2}(k;t) = nD_0\int\frac{d\mathbf{k}_1}{(2\pi)^3}F(k_1;t)F(p;t)\left[c(p)+\frac{[\mathbf{k}\cdot\mathbf{p}]^2}{k^2p}\frac{dc(p)}{dp}\right]^2 +nD_0\int\frac{d\mathbf{k}_1}{(2\pi)^3}v_{\mathbf{k}}(\mathbf{k}_1,\mathbf{p})F(k_1;t)F(p;t) \times\left[\frac{3\mathbf{k}\cdot\mathbf{p}}{kp}\frac{dc(p)}{dp}-\frac{[\mathbf{k}\cdot\mathbf{p}]^3}{k^3p^3}\frac{dc(p)}{dp}+\frac{[\mathbf{k}\cdot\mathbf{p}]^3}{k^3p^2}\frac{d^2c(p)}{dp^2}\right] +2nD_0\int\frac{d\mathbf{k}_1}{(2\pi)^3}v_{\mathbf{k}}(\mathbf{k}_1,\mathbf{p})\left[c(p)+\frac{[\mathbf{k}\cdot\mathbf{p}]^2}{k^2p}\frac{dc(p)}{dp}\right] \times F(k_1;t)\frac{\mathbf{k}\cdot\mathbf{p}}{kp}\partial_pF(p;t) +\frac{nD_0}{2}\int\frac{d\mathbf{k}_1}{(2\pi)^3}[v_{\mathbf{k}}(\mathbf{k}_1,\mathbf{p})]^2\left[\frac{1}{p}-\frac{[\mathbf{k}\cdot\mathbf{p}]^2}{k^2p^3}\right] \times\partial_pF(p;t)F(k_1;t) +\frac{nD_0}{2}\int\frac{d\mathbf{k}_1}{(2\pi)^3}[v_{\mathbf{k}}(\mathbf{k}_1,\mathbf{p})]^2\left[\frac{\mathbf{k}\cdot\mathbf{p}}{kp}\right]^2F(k_1;t)\partial_p^2F(p;t). \quad (27)$$

In Eqs. (26-27) $\mathbf{p}=\mathbf{k}-\mathbf{k}_1$ and $p=|\mathbf{k}-\mathbf{k}_1|$.

IV. ISOTROPIC APPROXIMATION

Along with the expansion of the full equation of motion (4), we also examined an expansion of an isotropic

approximation to Eq. (4). The isotropic approximation has the advantage of being slightly easier computationally, and it allows for calculation of the susceptibility at any q.

The isotropic approximation assumes that the susceptibility $\chi_{\mathbf{q}}(\mathbf{k};t)$ is independent of the angle between $\mathbf{q}$ and $\mathbf{k}$, $\chi_{\mathbf{q}}(\mathbf{k};t) \approx \chi_q^{\rm iso}(k;t)$. To derive an equation of motion for $\chi_q^{\rm iso}(k;t)$ one could start by substituting the isotropic approximation into the full equation of motion and then average the resulting equation over the angle between $\mathbf{q}$ and $\mathbf{k}$. We propose a slight modification of this procedure that results in an equation that is somewhat easier computationally:

$$\begin{aligned}
&\partial_t \chi_q^{\rm iso}(k;t) + \frac{D_0 k^2}{S(k)} \chi_q^{\rm iso}(k;t) \\
&+ \int_0^t dt' M^{\rm irr}(k;t-t') \partial_{t'} \chi_q^{\rm iso}(k;t') \\
&+ \int_0^t dt' M_q^{\rm iso}(k;t-t') \partial_{t'} \tilde{F}(k;q;t') \\
&= nD_0 k^2 S(0) c(k) F(k;t) \\
&+ S(0) \int_0^t dt' M^{\rm irr}(k;t-t') \partial_{t'} F(k;t'). \qquad (28)
\end{aligned}$$

where

$$\begin{aligned}
M_q^{\rm iso}(k;t) &= nD_0 \int \frac{d\mathbf{k}_1}{(2\pi)^3} \chi_q^{\rm iso}(k_1;t) F(|\mathbf{k}-\mathbf{k}_1|;t) \\
&\times v_{\mathbf{k}}(\mathbf{k}_1, \mathbf{k}-\mathbf{k}_1) \tilde{v}_{\mathbf{k}}(\mathbf{k}_1, \mathbf{k}-\mathbf{k}_1; q) \qquad (29)
\end{aligned}$$

and

$$\tilde{F}(k;q;t) = \int \frac{d\hat{\mathbf{q}}}{4\pi} F(|\mathbf{k}+\mathbf{q}|;t), \qquad (30)$$

$$\tilde{v}_{\mathbf{k}}(\mathbf{k}_1, \mathbf{k}-\mathbf{k}_1; q) = \int \frac{d\hat{\mathbf{q}}}{4\pi} \frac{k v_{\mathbf{k}+\mathbf{q}}(\mathbf{k}_1+\mathbf{q}, \mathbf{k}-\mathbf{k}_1)}{|\mathbf{k}+\mathbf{q}|}. \qquad (31)$$

Finally, the initial condition for $\chi_q^{\rm iso}(k;t)$ is

$$\chi_q^{\rm iso}(k;t=0) = S(k)S(q) \int \frac{d\hat{\mathbf{q}}}{4\pi} S(|\mathbf{k}+\mathbf{q}|). \qquad (32)$$

Note that in Eq. (28) we took the source term in the $q \to 0$ limit. The q dependence of the source term has very little effect on the size of the correlation length (see discussion in Sec. VI). Taking the source term in the $q \to 0$ limit makes the numerical calculation of $\chi_q^{\rm iso}(k;t)$ somewhat easier.

To get the characteristic length we expanded $\chi_q^{\rm iso}(k;t)$ in powers of q,

$$\begin{aligned}
\chi_q^{\rm iso}(k;t) &= \chi^{(0)}(k;t) + \frac{q^2}{2} \left[\frac{\partial^2 \chi_q^{\rm iso}(k;t)}{\partial q^2} \right]_{q=0} + \dots \\
&= \chi^{(0)}(k;t) + q^2 \chi^{\rm iso(2)}(k;t) + \dots . \qquad (33)
\end{aligned}$$

The zeroth order coefficient, $\chi^{(0)}(k;t)$, is the same as the one obtained from the expansion of the complete equation of motion. The equation of motion for $\chi^{\rm iso(2)}(k;t)$ can be readily obtained from Eq. (28):

$$\begin{aligned}
&\partial_t \chi^{\rm iso(2)}(k;t) + \frac{D_0 k^2}{S(k)} \chi^{\rm iso(2)}(k;t) \\
&+ \int_0^t dt' M^{\rm irr}(k;t-t') \partial_{t'} \chi^{\rm iso(2)}(k;t) \\
&+ \int_0^t dt' M_2^{\rm iso}(k;t-t') \partial_{t'} F(k;t') \\
&= -\frac{1}{6} \int_0^t dt' M_0^{\chi}(k;t-t') \partial_{t'} \partial_k^2 F(k;t') \\
&-\frac{1}{3k} \int_0^t dt' M_0^{\chi}(k;t-t') \partial_{t'} \partial_k F(k;t') \\
&-\frac{2}{3} \int_0^t dt' M_3^{\rm iso}(k;t-t') \partial_{t'} F(k;t') \qquad (34)
\end{aligned}$$

where

$$\begin{aligned}
&M_2^{\rm iso}(k;t) = \qquad (35) \\
&nD_0 \int \frac{d\mathbf{k}_1}{(2\pi)^3} [v_{\mathbf{k}}(\mathbf{k}_1, \mathbf{p})]^2 \chi^{\rm iso(2)}(k_1;t) F(|\mathbf{k}-\mathbf{k}_1|;t),
\end{aligned}$$

$M_0^{\chi}(k;t)$ is defined in Eq. (13), and

$$\begin{aligned}
&M_3^{\rm iso}(k;t) = \qquad (36) \\
&\frac{nD_0}{2} \int \frac{d\mathbf{k}_1}{(2\pi)^3} v_{\mathbf{k}}(\mathbf{k}_1, \mathbf{p}) F(p;t) \chi^{(0)}(k_1;t) \\
&\times \left[\frac{c(k_1)}{k} - \frac{v_{\mathbf{k}}(\mathbf{k}_1, \mathbf{p})}{k^2} + \frac{\mathbf{k}\cdot\mathbf{k}_1}{2k} \frac{d^2 c(k_1)}{dk_1^2} \right. \\
&\left. - \frac{2(\mathbf{k}\cdot\mathbf{k}_1)^2 - 2k^2 \mathbf{k}\cdot\mathbf{k}_1 - k^2 k_1^2}{k^3 k_1} \frac{dc(k_1)}{dk_1} \right].
\end{aligned}$$

In Eq. (36) $\mathbf{p} = \mathbf{k} - \mathbf{k}_1$ and $p = |\mathbf{k} - \mathbf{k}_1|$.

The initial condition to Eq. (34) is given by

$$\begin{aligned}
\chi^{\rm iso(2)}(k;0) &= \frac{S^2(k)}{2} \left[\frac{d^2 S(q)}{dq^2} \Big|_{q=0} \right] \qquad (37) \\
&+ \frac{S(0)S(k)}{3k} \frac{dS(k)}{dk} + \frac{S(0)S(k)}{6} \frac{d^2 S(k)}{dk^2}.
\end{aligned}$$

V. NUMERICAL EVALUATION OF $\chi^{(n)}(k;t)$

We numerically calculated the k and t dependence of $\chi^{(0)}(k;t)$, $\chi^{(1)}(k;t)$ and $\chi^{(2)}(k;t)$ using a previously developed algorithm that was designed to solve mode-coupling like equations [15, 16, 17]. The only input in this calculation is the static structure factor $S(k)$, which we calculated for the hard sphere interaction potential using the Percus-Yevick approximation. We report our results in terms of the relative distance from the ergodicity breaking transition predicted by mode-coupling theory, $\epsilon = (\phi_c - \phi)/\phi_c$. Here ϕ is the volume fraction,

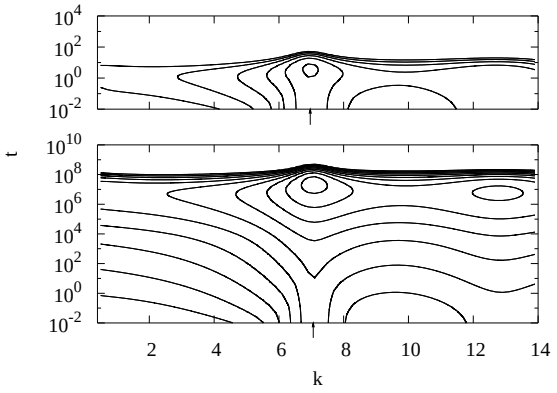

FIG. 1: Time and wave-vector dependence of $\mathbf{q} = 0$ value of three-point susceptibility, $\chi_{\mathbf{q}=0}(\mathbf{k};t) \equiv \chi^{(0)}(k;t)$ for the reduced distance from the mode-coupling transition, $\epsilon = (\phi_c - \phi)/\phi_c = 0.05$ (upper panel) and $\epsilon = 10^{-4}$ (lower panel). Contours correspond to $\chi^{(0)}(k;t) = 4^n$ where n is an integer, starting from $n = -6$. The arrow marks the position of the first peak of the static structure factor.

$\phi = n\pi\sigma^3/6$, where σ is the hard sphere diameter, and ϕ_c is the volume fraction at the mode-coupling transition. We used 300 equally spaced wave-vectors with spacing $\delta = 0.2$, between $k_0 = 0.1$ and $k_{\max} = 59.9$, and this discretization resulted in a mode-coupling transition at $\phi_c = 0.515866763$.

Shown in Fig. 1 are contour plots of $\chi^{(0)}(k;t)$ as a function of wave-vector k and time t for $\epsilon = 0.05$ and $\epsilon = 10^{-4}$. The former value of ϵ is the smallest relative distance from an avoided mode coupling transition in the Kob-Andersen binary mixture at which mode-coupling theory agrees with computer simulations [17]. As we mentioned earlier, $\chi^{(0)}(k;t)$ is proportional to the three-point susceptibility $\chi_n(k;t)$ calculated in Ref.[18], which is a mode-coupling approximation for the density derivative of the intermediate scattering function. Thus, all results derived in Ref.[18] for for $\chi_n(k;t)$ also apply to $\chi^{(0)}(k;t)$. In particular, there is a well defined maximum in $\chi^{(0)}(k;t)$ at a well defined wave-vector and at a characteristic time. Also, all the scaling laws observed for $\chi_n(k;t)$ apply to $\chi^{(0)}(k;t)$ (we show some of these scaling laws below). The characteristic wave-vector, $k_{\max}$, is nearly constant as the mode coupling transition is approached and $k_{\max} \approx 7.1$ close to the transition.

While the characteristic wave-vector is nearly constant close to the transition, the characteristic time grows rapidly as the mode-coupling transition is approached and diverges at the transition. In Fig. 2 we examine the time at which $\chi^{(n)}(k_{\max};t)$ is a maximum, $t^{(n)}_{\max}$, as a function of ϵ for the characteristic wave-vector $k_{\max} = 7.1$. We compare $t^{(n)}_{\max}$ with the α relaxation time τ_α, for which we use the standard definition $F(k_{\max};\tau_\alpha) = e^{-1}$. We find that $t^{(n)}_{\max}$ is slightly larger than τ_α, but has the same ϵ dependence, *i.e.* $t^{(n)}_{\max} \sim \epsilon^{2.46}$. Shown in the Fig. 2b are the ratios $t^{(n)}_{\max}/\tau_\alpha$, and it can be seen that these ratios are constant close to the mode-coupling transition. Thus, in the $\epsilon \to 0$ limit we see that $t^{(0)}_{\max} = 1.4\tau_\alpha$, $t^{(1)}_{\max} = 2.8\tau_\alpha$, and $t^{(2)}_{\max} = 1.4\tau_\alpha$. Notice that the peak of $\chi^{(0)}(k_{\max};t)$ and $\chi^{(2)}(k_{\max};t)$ occur at the same time.

Finally, in Fig. 3 we compare the values of $\chi^{(n)}(k_{\max};t)$ at $t^{(n)}_{\max}$. We find that $|\chi^{(0)}(k_{\max};t^{(0)}_{\max})|$ and $|\chi^{(1)}(k_{\max};t^{(1)}_{\max})|$ grow as ϵ^{-1} whereas $|\chi^{(2)}(k_{\max};t^{(2)}_{\max})|$ grows as $\epsilon^{-3/2}$. As we discuss in the next section, this disparate behavior of $\chi^{(n)}(k_{\max};t)$ is important for the existence of a diverging characteristic length.

We should note at this point that the ϵ dependence of $\chi^{(n)}(k;t)$ can be deduced from scaling predictions described in Ref. [13], and the numerical results presented here fully agree with the these predictions.

VI. DIVERGING CHARACTERISTIC LENGTH

To obtain a growing characteristic length scale as the mode-coupling transition is approached, we need $|\chi^{(n)}(k;t)|$ for some $n > 0$ to grow faster than $|\chi^{(0)}(k;t)|$ at a fixed time t. Then a diverging length can be calculated as $|\chi^{(n)}(k;t)/\chi^{(0)}(k;t)|^{(1/n)}$.

From Fig. 3 it is clear that the linear term, $\chi^{(1)}(k;t)$, does not result in a growing length scale. On the other hand, the absolute value of the isotropic second order term, $|\chi^{(2)}(k;t)|$, grows faster than $\chi^{(0)}(k;t)$ and thus we can define a diverging characteristic length $\xi(k;t)$,

$$\xi(k;t) = \sqrt{-\frac{\chi^{(2)}(k;t)}{\chi^{(0)}(k;t)}}, \tag{38}$$

where the negative sign comes from the observation that $\chi^{(2)}(k;t)$ is of opposite sign of $\chi^{(0)}(k;t)$ around τ_α and close to the transition. Note that for large times t, Eq. 38 involves a division of a small number by another small number. Because of numerical issues present in the algorithm to calculate $\chi^{(n)}(k;t)$, we only show results if $\chi^{(n)}(k;t) \geq 10^{-3}$, and therefore we, unfortunately, cannot comment at the asymptotic $t \to \infty$ limit of the characteristic length.

In Fig. 4 we examine $\xi(k_{\max};\tau_\alpha)$, *i.e.* the characteristic length at $k = k_{\max}$ and at the α relaxation time. The length $\xi(k_{\max};\tau_\alpha)$ grows as $\epsilon^{-1/4}$ and it reaches only 15 particle diameters at $\epsilon = 10^{-6}$. Thus the characteristic length is not very large even very close to the transition. For $\epsilon = 0.05$, we find that $\xi(k_{\max};\tau_\alpha)$ is only about one particle diameter. Note that Eq. (38) defines a length scale for every wave-vector k and at all times t, and we examine the time and wave-vector dependence of $\xi(k;t)$ below.

We determined that setting the initial condition for $\chi^{(2)}(k;t=0)$ to zero and/or taking $\mathcal{S}^{(2)}(k;t) = 0$ had very little effect on the size of the correlation length close to the mode-coupling transition. While including these

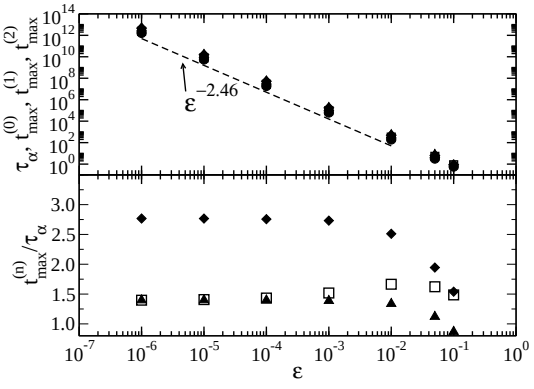

FIG. 2: Upper Panel: the α relaxation time, τ_α (filled circles), and the peak positions of $\chi^{(n)}(k_{\max};t)$, $\tau^{(n)}_{\max}$, as a function of $\epsilon = (\phi - \phi_c)/\phi_c$: $\tau^{(0)}_{\max}$–triangles; $\tau^{(1)}_{\max}$–diamonds; $\tau^{(2)}_{\max}$–open squares. Lower Panel: the ratio $\tau^{(n)}_{\max}/\tau_\alpha$ as a function of ϵ.

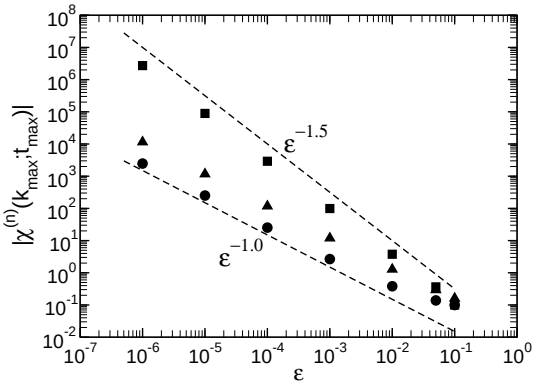

FIG. 3: The peak height of $\chi^{(n)}(k;t)$ as a function of the distance from the mode coupling transition ϵ. $\chi^{(0)}(k_{\max};t_{\max})$ – triangles; $\chi^{(1)}(k_{\max};t_{\max})$ – circles; $\chi^{(2)}(k_{\max};t_{\max})$ – squares

terms is in principle straightforward, dropping them significantly simplifies the numerical calculation.

Fourier transforms of four-point correlation functions, *i.e.* four-point dynamic structure factors, are often monitored in simulations and used to investigate properties of dynamic heterogeneities. Since the $q = 0$ value of a four-point structure factor should be proportional to the characteristic volume in which correlated motion takes place, an increase of the $q = 0$ value (*i.e.* of the height of four-point structure factor) is often given as evidence of an increase in a dynamic correlation length.

Similarly, for the problem considered here, the value of $\chi^{(0)}(k;t)$ could used as an indicator of the size of a characteristic dynamic range of the response. However, the spatial extent of dynamic response is best measured by examining the long-range spatial decay of a direct space

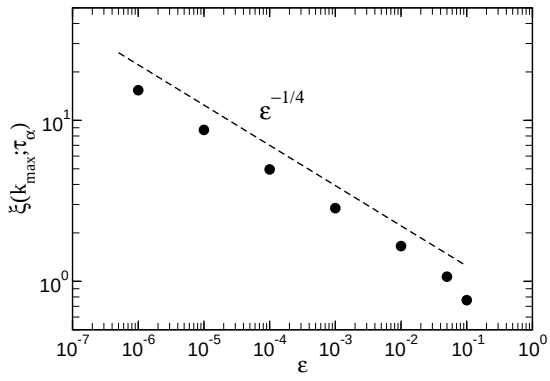

FIG. 4: The characteristic dynamic length $\xi(k_{\max};\tau_\alpha)$ as a function of the distance from the transition ϵ.

susceptibility or, alternatively, by examining the small-q behavior of the susceptibility $\chi_{\mathbf{q}}(\mathbf{k};t)$. This distinction is significant in view of the very strong wave-vector and time dependence of $\chi^{(0)}(k;t)$. In particular, if the characteristic length were a monotonic function of $\chi^{(0)}(k;t)$, then Fig. 1 would be leading to the unfortunate conclusion that $\xi(k;t)$ is a very strong function of k. The length would then have a rather limited appeal. In the following paragraph we show that this is not the case.

In Fig. 5 we compare the k dependence of $\xi(k;t)$ (right figure) and $\chi^{(0)}(k;t)$ (left figure) for three characteristic times: (1) early β (dotted line), late-β (dashed line), and at the α relaxation time (solid line). For reference, $F(k_{\max};t)$ is shown in the insert to Fig. 5 with the three characteristic times shown as vertical lines in the figure. There is a very strong dependence of $\chi^{(0)}(k;t)$ on k, but $\xi(k;\tau_\alpha)$ is nearly constant at each time. Therefore, even though there is a strong k dependence of the three-point susceptibility, there is a well defined characteristic dynamic length $\xi(k;t)$ that is independent of k and only depends on the time t. This suggests that we could drop the explicit k dependence of $\xi(k;t)$ and introduce a simplified notation $\xi(t)$.

Next, we investigate the time dependence of the characteristic length. Shown in Fig. 6 is $\chi^{(0)}(k_{\max};t)$ (lower curve-right axis), $|\chi^{(2)}(k_{\max};t)|$ (middle curve-right axis), and $\xi(t)$ (upper curve-left axis) as a function of time for $\epsilon = 10^{-6}$. The correlation length $\xi(t)$ is close to one for $t = 0$, begins to grow during β relaxation and reaches a plateau at a time corresponding to the late β-early α relaxation. During the α relaxation, $\xi(t)$ is approximately constant. Note that $\xi(t)$ has a very different time dependence than $\chi^{(0)}(k_{\max};t)$. Therefore, the length scale associated with dynamic heterogeneities are not a maximum when $\chi^{(0)}(k;t)$ is a maximum, but rather reaches a constant value for times less than this characteristic time.

Scaling relations for different time regimes can be de-

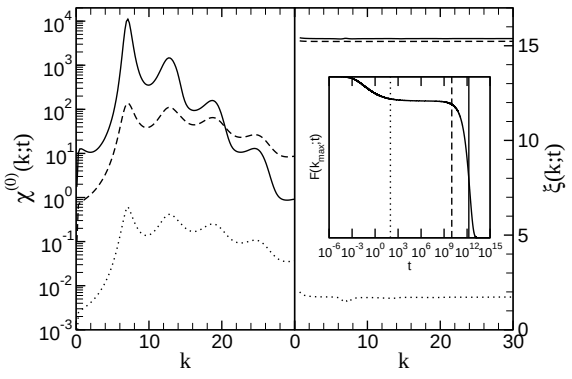

FIG. 5: Left panel: the wave-vector dependence of the $\mathbf{q} = 0$ value of the three-point susceptibility, $\chi_{\mathbf{q}=0}(\mathbf{k};t) \equiv \chi^{(0)}(k;t)$, at a time corresponding the the early β relaxation regime (dotted line), the late β regime (dashed line), and the α relaxation time (solid line). Right panel: the wave-vector dependence of the characteristic dynamic length $\xi(k;t)$ for the same times as in the left panel. The inset is the self-intermediate scattering function $F(k;t)$ and the three vertical lines correspond to the three times in left and right panels.

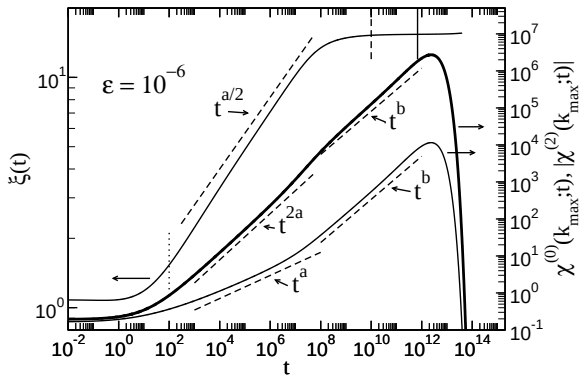

FIG. 6: The time dependence of the characteristic dynamic length $\xi(t)$ (left solid line and left axis), the susceptibility $\chi^{(0)}(k_{\max};t)$ (right solid line and right axis), and the second order coefficient $\chi^{(2)}(k_{\max};t)$ (middle, heavy solid line and right axis), showed on a log-log scale. The dashed lines show the scaling laws in the β relaxation regime. The vertical lines crossing $\xi(t)$ correspond to the three times shown in the inset to Fig. 5.

rived from the predictions of the mode coupling theory [8, 13]. Specifically, in the early β regime $\chi^{(0)}(k;t) \sim t^a$, and in the late β regime $\chi^{(0)}(k;t) \sim t^b$ where $a = 0.312$ and $b = 0.583$ for our system. The power law growth of $\chi^{(0)}(t)$ and $\chi^{(2)}(t)$ are also shown in Fig. 6. During the early β relaxation regime, $\chi^{(0)}(t) \sim t^a$ while $\chi^{(2)}(t) \sim t^{2a}$, which gives rise to the $t^{a/2}$ growth of the

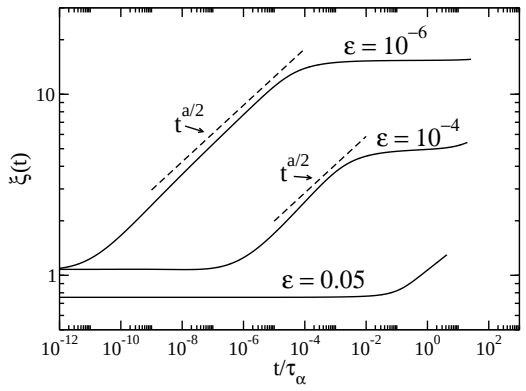

FIG. 7: The characteristic dynamic length $\xi(k_{\max};t)$ as a function of t/τ_α for $\epsilon = 0.05$, 10^{-4} and 10^{-6}. The dashed lines is the scaling law $\xi(t) \sim t^{a/2}$ valid in the β relaxation regime.

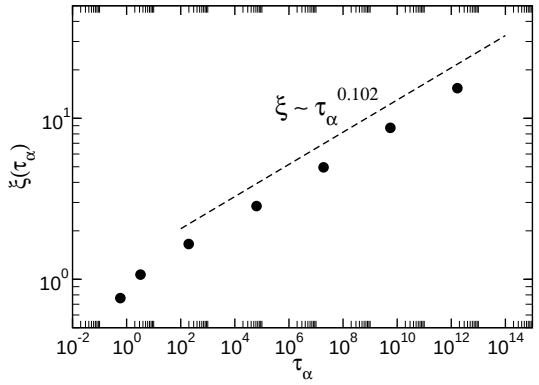

FIG. 8: The characteristic dynamic length $\xi(\tau_\alpha)$ calculated at the α relaxation time as a function of the α relaxation time.

correlation length in the early β relaxation regime. However, during late β relaxation, $\chi^{(2)}(t)$ and $\chi^{(0)}(t)$ both grow as t^b, thus there is no growing length scale. The vertical lines in the figure denote the same times as the vertical lines in the inset to Fig. 5.

In Fig. 7 we show $\xi(k_{\max};t)$ as a function of t/τ_α for $\epsilon = 0.05$, 10^{-4}, and 10^{-6}. For $\epsilon = 10^{-4}$ we observe the $t^{a/2}$ scaling for only a very narrow range of time, and we do not observe the $t^{a/2}$ scaling for any time range at $\epsilon = 0.05$, which suggests that it might be very difficult to see this scaling in simulations.

Finally, we note that since $\tau_\alpha \sim \epsilon^{-2.46}$ and $\xi \sim \epsilon^{-0.25}$, then $\xi \sim \tau_\alpha^{0.102}$, Fig. 8. As a result, a modest increase in the correlation length is accompanied by a very large increase of the relaxation time.

VII. NUMERICAL EVALUATION OF $\chi_q^{\rm iso}(k;t)$ AND ASSOCIATED CHARACTERISTIC LENGTH

The isotropic approximation neglects the dependence of the three-point susceptibility on the angle between **k** and **q**. Thus, in the resulting equation of motion for $\chi_q^{\rm iso}(k;t)$ q is just a parameter, and the equation of motion can be solved separately for any value of q. As a result, the full q dependence of $\chi_q^{\rm iso}(k;t)$ can be calculated. On the other hand, the isotropic approximation preserves the essential terms in the equation of motion which lead to the divergence of the $q \to 0$ limit of $\chi_q^{\rm iso}(k;t)$ and of the characteristic length. In this section we examine the isotropic approximation and compare this approximation to the expansion terms given above. Since the equations of motion are similar and the terms that cause the divergence are identical, many of the results of Sec. V carry over to the isotropic approximation. Notably, as we already noted in Sec. IV, $\chi^{(0)}(k;t)$ is identical in both cases.

Since we can calculate the whole q dependence in the isotropic approximation, we can determine the characteristic length $\xi(t)$ using two different methods. We can either evaluate $\chi_q^{\rm iso}(k;t)$ and then fit $\chi_q^{\rm iso}(k;t)/\chi^{(0)}(k;t)$ to $1-(\xi^{\rm iso}(k;t)q)^2$ for small q or we can determine $\xi^{\rm iso}(k;t)$ from $\sqrt{-\chi^{iso(2)}(k;t)/\chi^{(0)}(k;t)}$. Both methods result in the same length.

It can be showed that within the isotropic approximation the characteristic length is almost k-independent (and thus we will denote it by $\xi^{\rm iso}(t)$). In addition, the time dependence of the length is very similar to what was obtained from the full equations of motion in Sec. V.

In Fig. 9 we compare the magnitude of the characteristic length obtained from the isotropic approximation, $\xi^{\rm iso}(\tau_\alpha)$, with that following from the full equations of motion, $\xi(\tau_\alpha)$. As we anticipated in the first paragraph of this section, the isotropic approximation gives a length which diverges as $\epsilon^{-1/4}$. However, the isotropic approximation underestimates the characteristic length; for small ϵ the length resulting from the isotropic approximation is approximately 36% smaller than the length resulting from the expansion of the complete equation (4).

There has been some discussion in the literature as to what scaling function should be used to determine $\xi(t)$. According to the scaling relation presented in Ref. [13], in the β and α regimes the divergent part of $\chi_{\mathbf{q}}(\mathbf{k};t)$ is a function of a scaling variable $q\xi(t)$ only for small q close to the transition, $\chi_{\mathbf{q}}(\mathbf{k};t) = \mathcal{X}_{\beta,\alpha}(q\xi(t_{\beta,\alpha}),k)$. We use the isotropic approximation to examine some properties of scaling function $\mathcal{X}_{\beta,\alpha}$ close to the mode coupling transition, in the β and α regimes.

For times t in the vicinity of the β relaxation time τ_β, the scaling function $\mathcal{X}_\beta(q\xi(t_\beta),k)$ is predicted to have the Ornstein-Zernicke behavior, namely $\mathcal{X}_\beta(q\xi(t_\beta),k)$ should scale as q^{-2} for large q [13]. To check this prediction we first need to define the β relaxation time. We define τ_β as

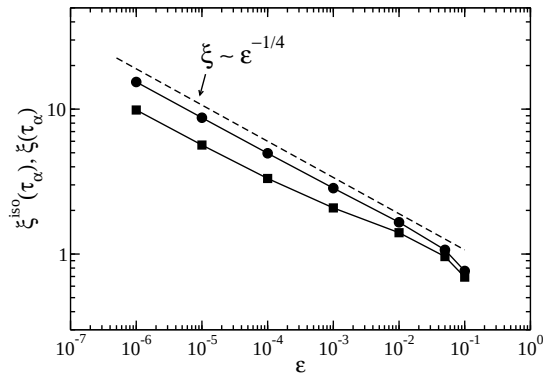

FIG. 9: The characteristic dynamic length $\xi^{\rm iso}(k;t)$ calculated using the isotropic approximation (squares) and without the isotropic approximation (circles).

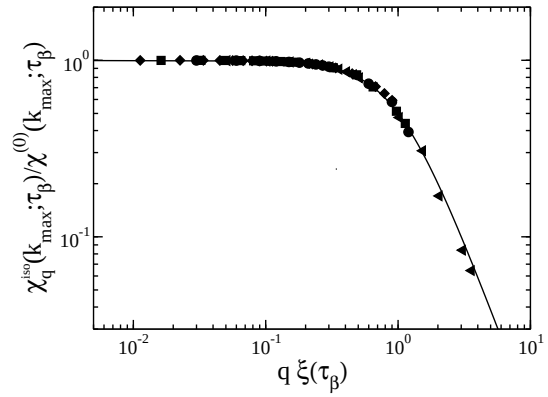

FIG. 10: The isotropic approximation for the dynamic susceptibility $\chi_q^{\rm iso}(k_{\rm max};\tau_\beta)$ as a function of $q\xi(\tau_\beta)$ for $\epsilon \le 10^{-3}$. Only data for q in the scaling regime are included. The solid line is the Ornstein-Zernicke function $1/[1+(\xi q)^2]$.

the inflection point of $F(t)$ versus $\ln(t)$. We verified that this definition agrees with the MCT scaling $\tau_\beta \sim \epsilon^{-1/2a}$. This time τ_β is only well defined for $\epsilon \le 10^{-3}$. Shown in Fig. 10 is $\chi_q^{\rm iso}(k_{\rm max};\tau_\beta)/\chi^{(0)}(k_{\rm max};\tau_\beta)$ as a function of $q\xi(\tau_\alpha)$ and the Ornstein-Zernicke function $1/[1+(\xi q)^2]$, which provides a good fit for small q during the β relaxation time and demonstrates the q^{-2} scaling for large q.

For times t comparable to the α relaxation time τ_α, the inhomogeneous mode-coupling theory [13] predicts a q^{-4} behavior of the scaling function $\mathcal{X}_\alpha(q\xi(t_\alpha),k)$at large q. We test this prediction in Fig. 11: we show $\chi_q^{\rm iso}(k_{\rm max};\tau_\alpha)/\chi^{(0)}(k_{\rm max};\tau_\alpha)$ as a function of $q\xi(\tau_\alpha)$ along with two functions commonly used to find $\xi(t)$ in simulations, and a function suggested by the inhomogeneous mode-coupling theory. The functions $1-(\xi q)^2$ (dotted

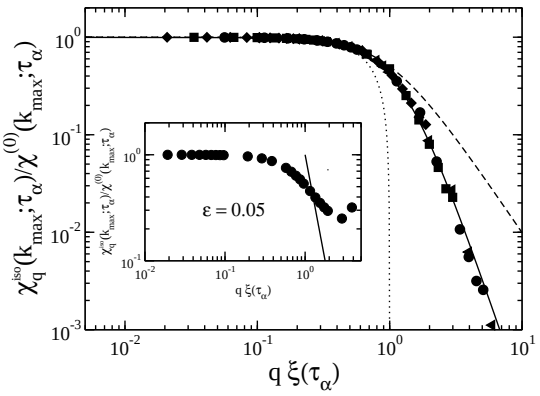

FIG. 11: The isotropic approximation for the dynamic susceptibility $\chi_q^{\rm iso}(k_{\rm max};\tau_\alpha)$ as a function of $q\xi(\tau_\alpha)$ for $\epsilon \leq 10^{-3}$. Only data for q in the scaling regime are included. The dotted line is $1-(q\xi)^2$, the dashed line is $1/[1+(q\xi)^2]$. The solid line is a fit to the data to a function of the form $1/[1+(q\xi)^2+a(q\xi)^4]$ where $a = 0.45$. The q^{-4} scaling for large q is evident. Inset: the dynamic susceptibility $\chi_q^{\rm iso}(k_{\rm max};\tau_\alpha)$ for $\epsilon = 0.05$ showing all the data including q values beyond the scaling regime. The inset shows that the q^{-4} scaling (solid line) is not apparent for this ϵ.

line) and the Ornstein-Zernicke function, $1/(1+[\xi q]^2)$, (dashed line) are good fits only to a very narrow q range, with the Ornstein-Zernicke function being a better fit for a larger range of q values. On the other hand, the function $1/[1+(\xi q)^2+a(\xi q)^4]$ where $a = 0.45$ (solid line), provides a good fit over a large q range and thus it confirms the q^{-4} scaling predicted by the inhomogeneous mode-coupling theory for the α relaxation time scale. Note that the q^{-4} scaling is not evident for $\epsilon = 0.05$ (inset), which suggests that this scaling might be difficult to observe in simulations.

VIII. CONCLUSIONS

We used inhomogeneous mode-coupling theory to numerically investigate the dynamic susceptibility $\chi_{\mathbf{q}}(\mathbf{k};t)$ at small q and determined time, k, and distance from the transition dependence of the diverging characteristic length scale. We confirmed scaling predictions presented in Ref. [13] and obtained a couple of new interesting results. Because of numerical issues, we were not able to calculate the asymptotic long time behavior of the diverging characteristic length scale. This would be an interesting topic that we leave for later analysis. It most likely requires an analytical argument that goes beyond the scaling analysis presented in Ref. [13].

The most important result of our numerical investigation is that the diverging characteristic length is very weakly k dependent. This makes it a well defined quantity. We speculate that the k independence of the characteristic length should carry over to the dynamic correlation length defined in terms of a four-point structure factor. Moreover, it should explain why a variety of slightly different four point functions (*e.g.* defined in terms of overlap functions [5, 19, 20] or in terms of self-intermediate scattering functions [6, 7, 21]) result in comparable dynamic correlation lengths.

The second important result, which cannot be obtained from scaling considerations alone, is the magnitude of the characteristic length. On general grounds we expect this length to be comparable to dynamic correlation lengths defined through four-point structure factors. Thus, it is satisfying that the magnitude of the length is indeed comparable (albeit somewhat smaller) to what's found in simulations.

We would like to point out that, although various simulations found comparable values of the dynamic correlation length, there are a few important unresolved differences between results obtained by different groups that preclude declaring that the characteristic length discussed in this work is essentially the same as the dynamic correlation length measured in simulations.

First, while the characteristic length defined through the three-point susceptibility is a monotonic function of time (at least as long as our numerical routines are reliable), the simulational results very. Lacevic *et al.* [5] found that the dynamic correlation length roughly followed the overall magnitude of the four-point correlation function and decayed to zero at later times. In contrast, Toninelli *et al.* [7] found that the dynamic correlation length continued to grow at later times. While slightly different fitting procedures were used in these two works, it is difficult to pinpoint the exact source of two strikingly different results.

Second, within the mode-coupling approximation, the characteristic length defined through the three-point susceptibility diverges as $\epsilon^{-1/4}$ upon approaching the ergodicity breaking transition predicted by the mode-coupling theory. We feel that the relevance of this result to simulations (and experiments) in which the mode-coupling transtion is avoided still needs to be fully established. We speculate that it is possible that in computer simulations a vestige of a power law divergence of the dynamic correlation length could be seen just as one can observe in simulations power law dependencies of various transport coefficients upon approaching a mode-coupling crossover [17]. Indeed, various groups have already claimed power law dependencies of their dynamic correlation lengths upon approaching the mode-coupling crossover (see, *e.g.* [6, 19, 20, 21, 22]). However, there seems to be some disagreement regarding the value of the scaling exponent and only one work, [19], results in a value agreeing with the prediction of the inhomogeneous mode-coupling theory. Upon closer examination of the fitting procedure described in Ref. [23] and re-examining our own simulation data we concluded that virtually all systems studied in simulations were not large enough to obtain the dynamic correlation length in a range allowing for an unambiguous

determination of the scaling exponent.

IX. ACKNOWLEDGMENT

We would like to thank G. Biroli, K. Miyazaki and D. Reichman for comments about this work. We gratefully acknowledge the support of NSF Grant No. CHE 0517709.

[1] M. Ediger, Annu. Rev. Phys. Chem. **51**, 99 (2000).
[2] R. Richert, J. Phys.: Condens. Matter **14**, R703 (2002).
[3] H. Andersen, Proc. Natl. Acad. Sci. U.S.A. **102**, 6686 (2005).
[4] N. Lacevic, F. Starr, T. Schroder, V. Novikov, and S. Glotzer, Phys. Rev. E **66**, 030101(R) (2002).
[5] N. Lacevic, F. Starr, T. Schroder, and S. Glotzer, J. Chem. Phys. **119**, 7372 (2003).
[6] L. Berthier, Phys. Rev. E **69**, 020201(R) (2004).
[7] C. Toninelli, M. Wyart, L. Berthier, G. Biroli, and J. Bouchaud, Phys. Rev. E **71**, 041505 (2005).
[8] L. Berthier, G. Biroli, J. Bouchaud, W. Kob, K. Miyazaki, and D. Reichman, J. Chem. Phys. **126**, 184503 (2007).
[9] F. Lechenault, O. Dauchot, G. Biroli, and J. Bouchaud, Europhys. Lett. **83**, 46002 (2008).
[10] F. Lechenault, O. Dauchot, G. Biroli, and J. Bouchaud, Europhys. Lett. **83**, 46003 (2008).
[11] L. Berthier, G. Biroli, J. Bouchaud, L. Cipelletti, D. Masri, D. L'Hote, F. Ladieu, and M. Pierno, Science **310**, 1797 (2005).
[12] C. Dalle-Ferrier, C. Thibierge, C. Alba-Simionesco, L. Berthier, G. Biroli, J. Bouchaud, F. Ladieu, D. L'Hote, and G. Tarjus, Phys. Rev. E **76**, 041510 (2007).
[13] G. Biroli, J. Bouchaud, K. Miyazaki, and D. Reichman, Phys. Rev. Lett. **97**, 195701 (2006).
[14] G. Szamel, unpublished.
[15] M. Fuchs, W. Gotze, I. Hofacker, and A. Latz, J. Phys.: Condens. Matter **3**, 5047 (1991).
[16] K. Miyazaki, B. Bagchi, and Yethiraj, cond-mat/0405326v1. Note that the published version of this manuscript [J. Chem. Phys. **121**, 8120 (2004)] does not contain the detailed description of the numerical algorithm.
[17] E. Flenner and G. Szamel, Phys. Rev. E **72**, 031508 (2005).
[18] G. Szamel and E. Flenner, Phys. Rev. E **79**, 021503 (2009).
[19] R. Stein and H. Andersen, Phys. Rev. Lett. **101**, 267802 (2008).
[20] S. Karamakar, C. Dasgupta, and S. Sastry, PNAS **106**, 3675 (2009).
[21] E. Flenner and G. Szamel, Phys. Rev. E **79**, 051502 (2009).
[22] S. Whitelam, L. Berthier, and J. Garrahan, Phys. Rev. Lett. **92**, 185705 (2004).
[23] R. Stein, Ph.D. thesis, Stanford University (2007).